Influence of microstructure and surface topography on material removal by the Hirtisation® process

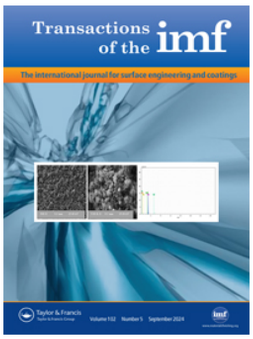

Taylor & Francis
Taylor & Francis Group

Transactions of the IMF

The International Journal of Surface Engineering and Coatings

ISSN: (Print) (Online) Journal homepage: www.tandfonline.com/journals/ytim20

Influence of microstructure and surface topography on material removal by the Hirtisation® process

Rasmus Gunnerek, Gowtham Soundarapandiyan, Michael Christoph Doppler, Eduard Hryha & Uta Klement

To cite this article: Rasmus Gunnerek, Gowtham Soundarapandiyan, Michael Christoph Doppler, Eduard Hryha & Uta Klement (22 Oct 2024): Influence of microstructure and surface topography on material removal by the Hirtisation® process, Transactions of the IMF, DOI: 10.1080/00202967.2024.2411903

To link to this article: https://doi.org/10.1080/00202967.2024.2411903

Published online: 22 Oct 2024.

TRANSACTIONS OF THE IMF
https://doi.org/10.1080/00202967.2024.2411903

Influence of microstructure and surface topography on material removal by the Hirtisation® process

Rasmus Gunnerek[a], Gowtham Soundarapandiyan[a], Michael Christoph Doppler[b], Eduard Hryha[a] and Uta Klement [a]

[a]Industrial and Materials Sciences, Chalmers University of Technology, Gothenburg, Sweden; [b]RENA Technologies Austria GmbH, Wiener Neustadt, Austria

ABSTRACT

The Hirtisation® process is an electro-chemical process, wherein the electrolyte can easily access both external and internal surfaces. The process shows promising results in both support structure removal and reduction of surface roughness, and has the potential to solve the productivity and quality trade-off in powder bed fusion – laser beam (PBF-LB) processing. In this study, the role of the microstructure and surface topography on the capability of the Hirtisation® process to lower the PBF-LB produced surface roughness, has been investigated. A detailed microstructure analysis by SEM was used to determine the effect of the Hirtisation® process on removal of sintered powder, the effects on melt pool boundaries and grain boundaries, and thus the final surface quality. The Hirtisation® process significantly reduced surface roughness thanks to the complete removal of sintering powder from the as-built surface. Additionally, preferential material removal was detected along melt pool boundaries, leading to creation of notches of up to 10 µm in depth.

ARTICLE HISTORY
Received 4 September 2024
Accepted 19 September 2024

KEYWORDS
Hirtisation; powder bed fusion–laser beam (PBF-LB); as-built microstructure; additive manufacturing (AM); stainless steel; post processing; surface topography; scan rotation

Introduction

Powder bed fusion – laser beam (PBF-LB) is the most popular powder-based metal additive manufacturing technology that enables the production of complex geometries that are either too expensive or not possible using conventional manufacturing processes such as turning or milling, etc. Design freedom has become interesting for applications in aerospace, energy and automotive industries. This is due to the almost unlimited design freedom that allows us to decrease components weight and functionality and hence improve overall performance.[1] However, the process is associated with relatively high surface roughness (R_a ~3–50 µm) in as-built state,[2] which requires surface improvement, especially for applications with high dynamic properties.[3] The tendency for crack formation under fatigue loading increases with increasing surface roughness and thus shortens the service life.[2] Hence, post processing is usually required to enhance the surface integrity.

During the PBF-LB process, metal powder is selectively melted and solidified under highly dynamic conditions by a fine laser where powder particles surrounding the solidified part can adhere to the surface of the component, generating unique surface topography.[4] Since the metal powder has a lower thermal conductivity than the solidified part, geometry changes along the build direction alter the heat dissipation through the part, which can lead to differences in microstructure[5,6] and surface topography.[7] The surface morphology of the solidified melt tracks is highly sensitive to variations in key printing parameters. Instabilities, such as those induced by the Plateau-Rayleigh instability and the Marangoni effect, can result in different concentrations of defects and fluctuations in surface waviness.[8] These instabilities manifest as balling, humps and laser ripples on the melt tracks and thus the final surface topography.

There are several post processing methods available today such as machining, shot-peening, sand blasting and chemical milling.[7] However, these processes have limitations when it comes to complex geometries. Internal structures require expensive special tools or are not accessible. Different strategies have been applied to reduce surface roughness where one aspect focuses on the impact of process parameters on the surface roughness during PBF-LB, such as changing the scan rotation and applying a contour, etc.[9]. Others are investigating new post-processes with the possibility of satisfying the demands of complex AM parts.[7] The relatively novel Hirtisation® process is a chemical and electrochemical process specifically designed for the needs of PBF-LB and other additive manufacturing (AM) processes, where the electrolyte can easily access both external and internal surfaces. The process has shown promising results in both support structure removal and surface enhancement.

Despite its potential, research on the Hirtisation® process remains limited, both in terms of materials and additive manufacturing (AM) processes explored. Sandell *et al.* observed that the surface roughness of Ti6Al4V produced *via* powder bed fusion – electron beam (PBF-EB) was significantly reduced from approximately 20 µm to 5 µm S_a after Hirtisation®.[10] They also highlighted the importance of controlling the amount of material removal to avoid eliminating essential surface contours or exposing sub-surface porosity. Controlling material removal was also highlighted in a study on Hirtisation® of AlSi10Mg by Beevers *et al.*[11]. They found that the coarsening of surface/subsurface grains during annealing needed full removal to improve fatigue life. Berglund *et al.* conducted a comprehensive study on the surface topography of Ti6Al4V before and after Hirtisation®. Their findings revealed that surface roughness (S_a) could be reduced by

CONTACT Rasmus Gunnerek rasmus.gunnerek@chalmers.se Industrial and Materials Sciences, Chalmers University of Technology, Gothenburg, Sweden

78%, mainly due to the reduction of deep valleys and the smoothing of peaks.[12]

Further demonstrating the process feasibility, Oosterbeek *et al.*[13] showed that Hirtisation® effectively reduced variations in lattice structure thickness for PBF-LB produced Ti6Al4V, decreasing roughness from 12 to 6 µm (S_a) and improved fatigue performance by removing sintered powder from the lattice surface. Interestingly, few studies on Hirtisation® and 316L stainless steel which is one of the most studied alloys for PBF-LB, have been performed. Que *et al.* compared the impact of various surface treatments and heat treatments on stress corrosion cracking behaviour where Hirtisation®, shot peening and polishing were compared. They found that the Hirtisation® process of solution annealed 316L stainless steel revealed the grain boundaries at the surface.[14]

While these studies present encouraging results in roughness reduction for AM-produced surfaces, they did not investigate in detail the influence of microstructural features at the surface. These features are expected to significantly impact the chemical or electrochemical material removal processes during Hirtisation®. PBF-LB is a complex process where slight variations in scanning strategy, component design and process parameters can yield significant differences in as-built microstructure and surface features even for the same machine. It is therefore important to understand how novel post processes such as the Hirtisation® interacts with PBF-LB surfaces and microstructure.

The aim of this work was to show how surface topography and microstructure influence the material removal by Hirtisation® of 316L stainless steel. Therefore, distinct differences in surface microstructure were generated by altering the scan strategy from a reference condition using standard process parameters as described in more detail in the next section. A state-of-the-art scan rotation of 67° without contour parameter was compared to conditions of 0° scan rotation as it yields significant differences in surface microstructure.[15]

Materials and methods

Powder feedstock and sample manufacturing

Gas atomised 316L stainless steel powder was supplied by Höganäs AB with a powder size distribution of 20–53 µm and chemical composition summarised in Table 1.

To investigate the influence of microstructure on material removal during the Hirtisation® process, state-of-the-art 67° rotation was compared to 0° scan rotation. Hence, cubes of $15 \times 15 \times 15$ mm^3 were manufactured in an EOS M290 apparatus using standard parameters for 40 µm layer thickness by EOS GmbH (316L_040_FlexM291_1.00) with a 67° scan rotation. A second set of cubes based on the standard parameters was produced, but without applying scan rotation. As illustrated in Figure 1(a), the 0° scan rotation creates a more anisotropic microstructure.

Hirtisation®

The samples were subjected to Hirtisation® post processing, a combination of both chemical and electrochemical processes by RENA Technologies Austria.[16] The Hirtisation® process is precisely tailored to the specific requirements of different alloy systems in terms of chemistry and the number of steps required. The general workflow of Hirtisation® is presented in Figure 1(b).

Table 1. Powder chemical composition wt.%.

	C	Ni	Cr	Mo	Mn	Si	O	Fe
AISI 316L	0.028	12.6	16.9	2.5	1.5	0.7	0.056	Balance

Surface characterisation

As-built samples were removed from the build plate by electric discharge machining and surface topography measurements were done before and after Hirtisation®. Selected areas of 2188×1645 µm were studied using Sensofar S neox-optical profilometer suitable for characterisation of AM surfaces.[17] Specific surface texture parameters were chosen and compared (S_a, S_z, S_{tr}, S_{dr} and S_{pd}) in accordance with the ISO 25178-2 standard.[18]

Microstructural characterisation

To study the influence of microstructure on material removal by the Hirtisation® process, samples were electrochemically etched in 10% oxalic acid to reveal features such as melt pool and grain boundaries. The characterisation of the part surface and microstructure before and after Hirtisation® was performed by combining light microscopy (LOM) and scanning electron microscopy (SEM) using a Zeiss Axioscope 7 optical microscope and a Zeiss Gemini 450 field emission scanning electron microscope.

Results and discussion

Impact of scan rotation on the as-built surfaces

The scan rotation determines how the building blocks, i.e. melt pools and melt tracks, combine during the PBF-LB process and thus influence the final surface and microstructure. To achieve a uniform surface and microstructure, the 67° scan rotation is preferred as it maximises the number of layer rotations before scan vectors return to the initial position.

Figure 2 shows the as-built surface for the 67° scan rotation at different magnifications along the build direction (BD). The surface topography image in Figure 2(a) shows that the roughness is due to adhered powder particles. SEM images (Figure 2(b and c)) confirm the presence of sintered or semi sintered particles on the surface but also the typical waviness created by the melt pools.[7] As can be seen, the particles can be found at different depths, with some settled in valleys formed by overlapping melt pools or adhered to the melt pools outer surface generating peaks in the surface topography scan in Figure 2(a).

With the 0° scan rotation, shown in Figure 3, the scan vectors remain aligned between layers, forcing the start and end of melt tracks to occur along the same axis. This results in anisotropic surface topography as seen in Figure 1(a), where surfaces perpendicular to the scan vectors (BD-Y), differ significantly from the (BD-X) surface. This is reflected in the roughness measurements (Table 2) where the BD-Y cross-section (Figure 3(a)) revealed a higher S_a of ~16 µm compared to the S_a of ~13 µm of the BD-X cross-section (Figure 3(d)). The greater roughness of the BD-Y cross-section can be explained by the fact that more powder is adhered to the surface (Figure 3(b and c)) than on the BD-X

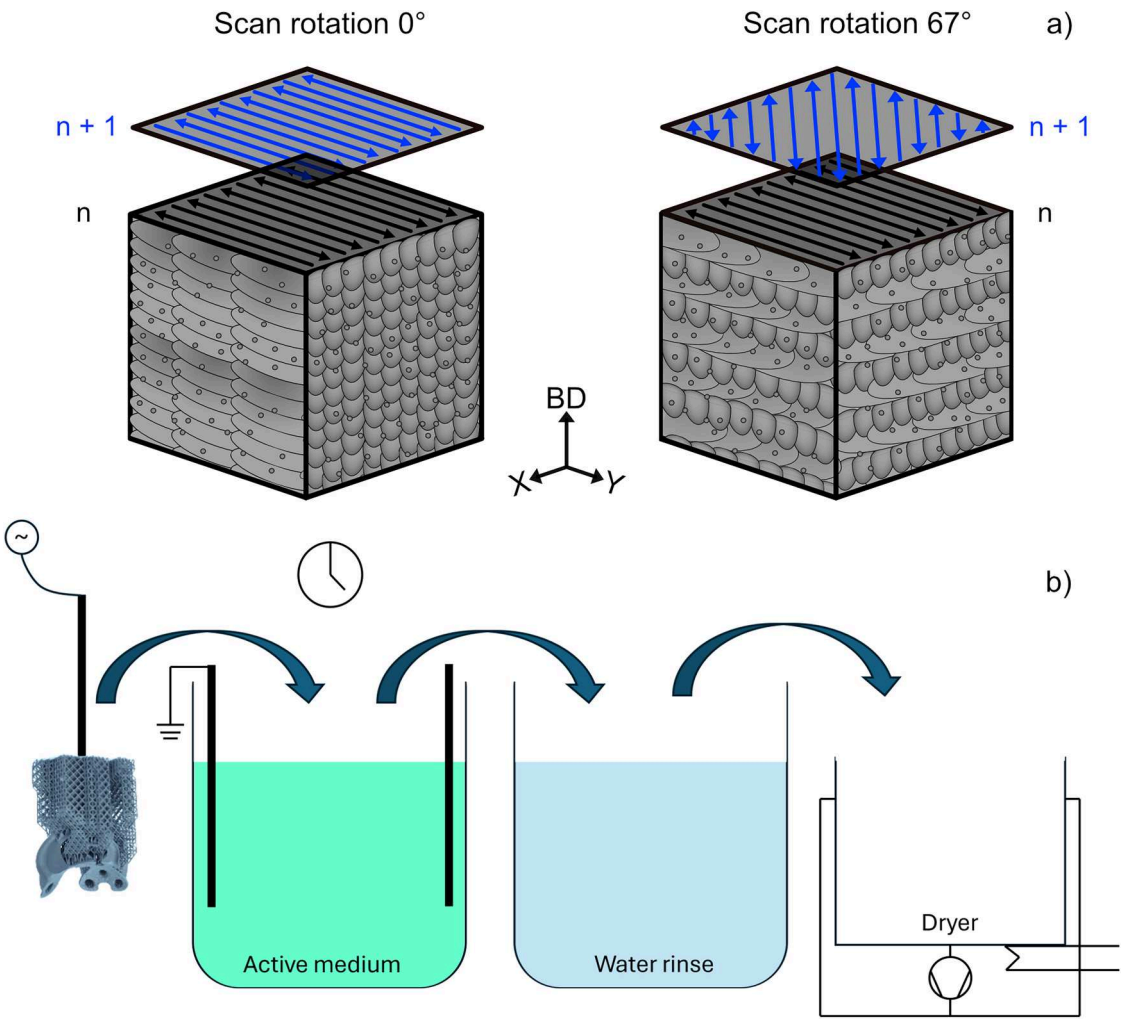

Figure 1. Schematic representation of the effect of (a) scan rotation on melt pool and melt tracks at 0° and 67° scan rotation. General workflow (b) for Hirtisation® with one active step. The part is contacted and immersed in the active medium, where material is removed over time. When the target condition is achieved, the part is rinsed and dried.

surface (Figure 3(e and f)). The 0° scan rotation does not only result in roughness differences but also in a clear anisotropy of the surface pattern. The stacking of melt pools (Figure 3(b)) generates valleys between overlapping melt pools, creating a pattern parallel to the build direction. The opposite is observed in Figure 3(d), where valleys created by the stacking of melt tracks show a surface pattern perpendicular to the build direction. Thus, clear anisotropic surface features with different roughness and surface patterns are present when using 0° scan rotation compared to 67° scan rotation. Therefore, the scan rotation sets different starting conditions for post processing applied to the as-built surfaces.

The surface topography values presented in Table 2 reflect the observed differences, with the arithmetic mean height (S_a) being higher for both investigated surfaces at a 67° scan rotation. Notably, the BD-X cross-section at a 0° scan rotation exhibits the largest deviation across all parameters in Table 2 when compared to the other measured surfaces. This cross-section recorded the lowest values for all parameters except for peak density (S_{pd}), which represents the

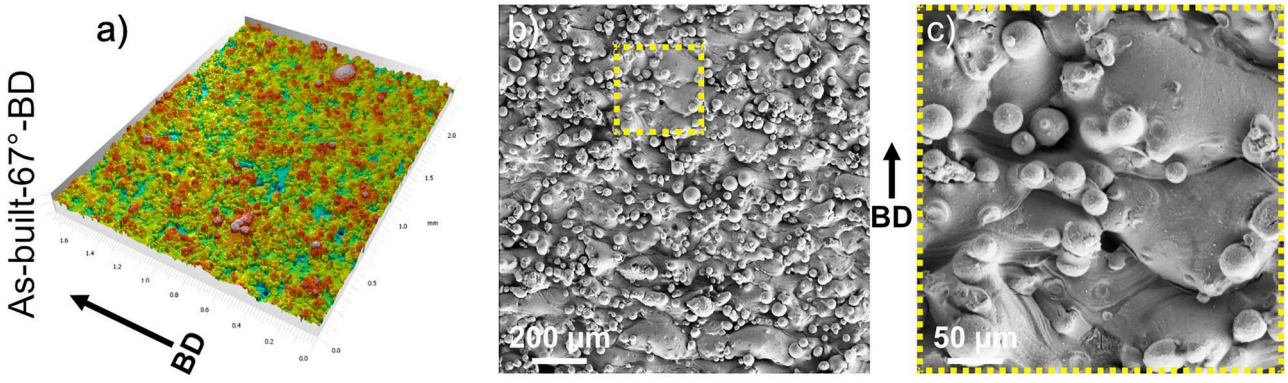

Figure 2. Surface topography of as-built surfaces using 67° scan rotation: (a) 3D surface image used for roughness measurements, and (b and c) SEM images taken at different magnifications showing surface features along the build direction.

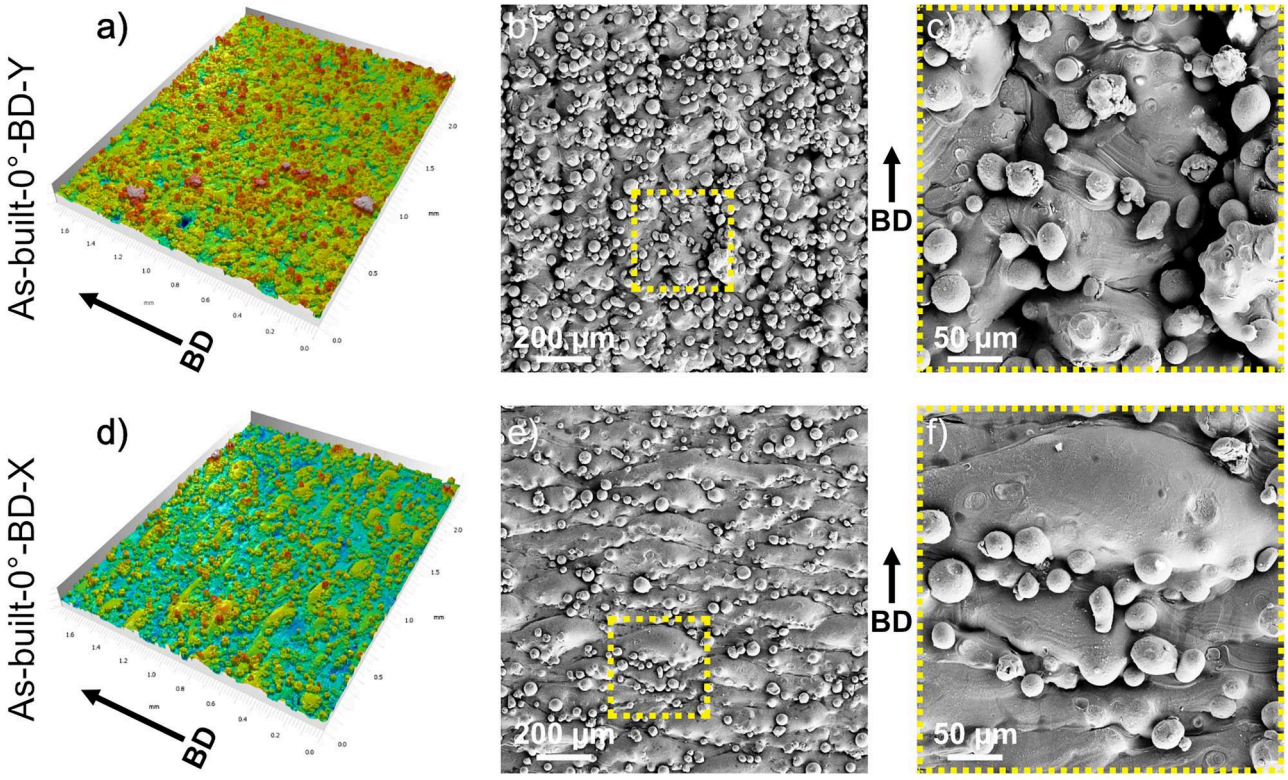

Figure 3. Surface topography of as-built surfaces using 0° scan rotation: (a) and (d) 3D surface image used for roughness measurements and (b), (c), (e), and (f) SEM images at different magnifications revealing surface features along the build direction.

number of peaks per mm^2. As highlighted in Figure 3, less powder was observed on this cross-section, suggesting that the instrument might have difficulty detecting the smallest powder particles on the other cross-sections.

Effect of scan rotation on Hirtisation®

After the Hirtisation® process, 3D roughness measurements and SEM analyses showed a reduction in surface roughness from 20 to 7 µm S_a for the 67° scan rotation, see Table 3. Figure 4(a) reveals a decrease in peak density from ~150 to 19 peaks per mm^2 compared to the as-built condition, with the presence of spherical features indicated by the blue colour. The SEM images in Figure 4(b and c) confirm the complete removal of powder particles that were attached to the surface. Melt pool boundaries and columnar grain boundaries are clearly etched during the Hirtisation® process.

The anisotropic surface pattern observed in the as-built sample remains after Hirtisation® of the sample with 0° scan rotation. Despite the reduction in roughness to approximately S_a~7 µm for the BD-Y cross-section, a more pronounced pattern emerges due to the powder removal between overlapping melt pools, resulting in a repeating pattern along the build direction (Figure 5(a)). This contrasts with the more randomly distributed spherical features seen in the sample with 67° scan rotation (Figure 4(a)). Analysis of the BD-X cross-section, which had the lowest roughness (S_a~5 µm) after Hirtisation®, shows that preferential etching of the melt track boundaries occurred, creating a fine pattern perpendicular to the build direction. Compared to the sample with 67° scan rotation, the SEM images of the sample with 0° scan rotation are free of visible traces of powder removal. This suggests that variations in as-built roughness and powder content within the same component can lead to significant differences in the surface pattern and features present after Hirtisation®.

These differences are further quantified in Table 3, where both the developed surface area (S_{dr}) and the texture aspect ratio (S_{tr}) are lower for the BD-X cross-section using the 0° scan rotation. Notably, all roughness parameters, including peaks per unit area (S_{pd}), recorded their lowest values for the BD-X cross-section. This is likely due to the improved accuracy of the measurements, facilitated by the removal of hard-to-distinguish fine powder from the as-built surfaces.

Role of microstructure on Hirtisation®

In the previous section, it was shown that the as-built surfaces can lead to macroscopic features on the surface after Hirtisation®. This section focuses on a deeper analysis of the surface microstructure before and after Hirtisation®. As described by Leicht *et al.*,[6] the state-of-the-art scan rotation of 67°produces an isotropic/random microstructure, while the 0° rotation

Table 2. Surface roughness measurements as-built conditions.

Condition	Cross-section	S_a (µm)	S_z(µm)	S_{dr} (%)	S_{tr}	S_{pd}(1 mm^{-2})
As-built-67°	BD-Y	17.5	185.7	119.0	0.88	168.5
As-built-67°	BD-X	19.2	212.5	130.5	0.88	130.5
As-built-0°	BD-Y	15.9	209.9	111.6	0.90	157.9
As-built-0°	BD-X	12.5	131.2	83.0	0.51	221.2

Table 3. Surface roughness measurements after Hirtisation®.

Condition	Cross-section	S_a(µm)	S_z(µm)	S_{dr} (%)	S_{tr}	S_{pd}(1 mm^{-2})
Hirtisation®-67°	BD-Y	7.0	76.0	4.7	0.63	17.5
Hirtisation®-67°	BD-X	7.4	75.7	5.6	0.73	19.9
Hirtisation®-0°	BD-Y	6.6	79.5	5.5	0.59	14.1
Hirtisation®-0°	BD-X	5.3	65.9	1.9	0.46	12.0

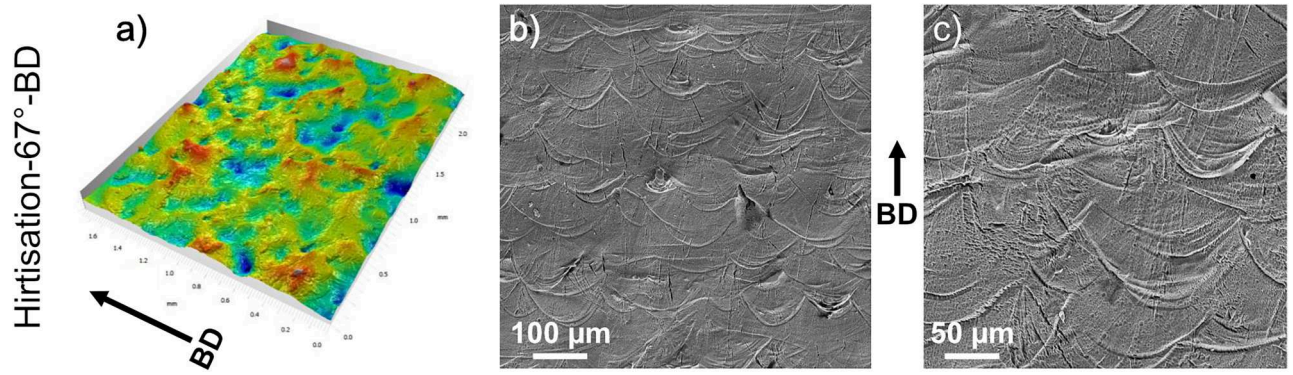

Figure 4. Surface topography after Hirtisation® when using 67° scan rotation: (a) 3D surface image used for roughness measurements, and SEM images (b) and (c) revealing surface features along the build direction.

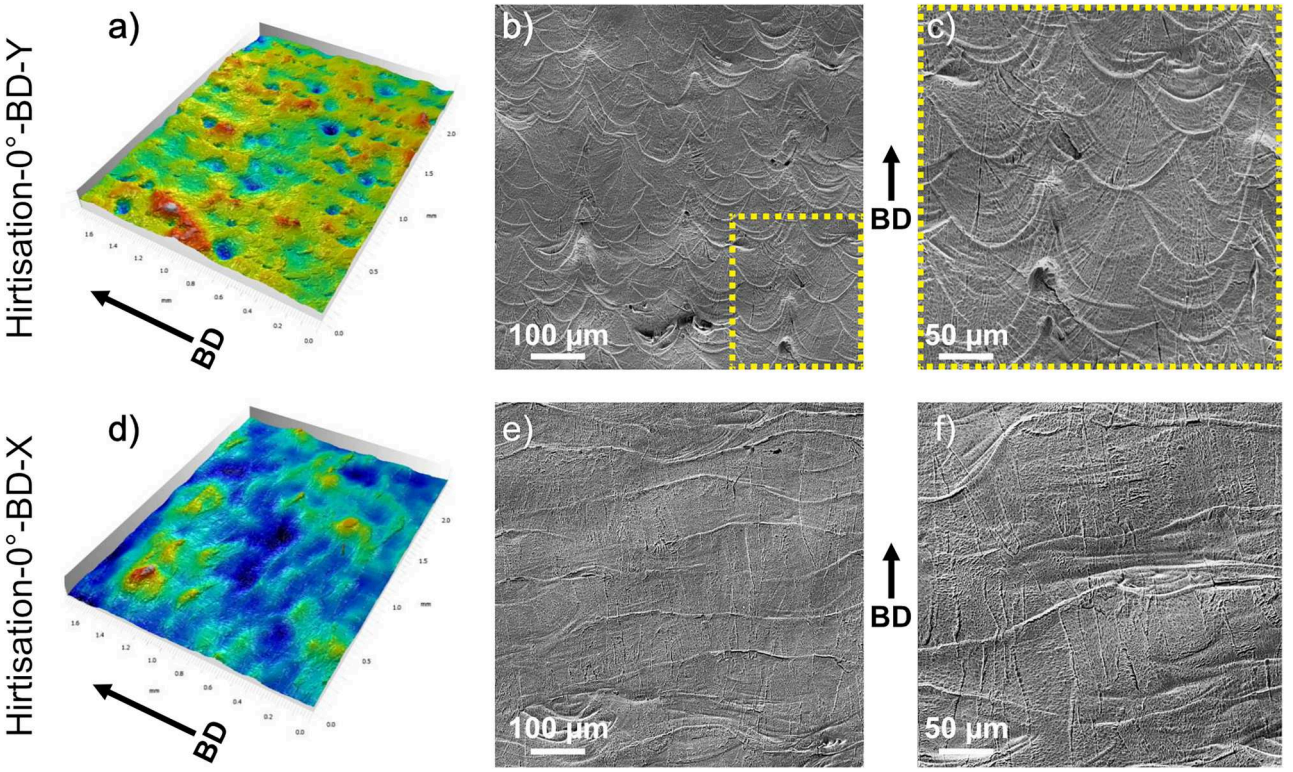

Figure 5. Surface topography after Hirtisation® when using 0° scan rotation: (a) and (d) 3D surface image used for roughness measurements and (b), (c), (e), and (f) SEM images at different magnifications revealing surface features along the build direction.

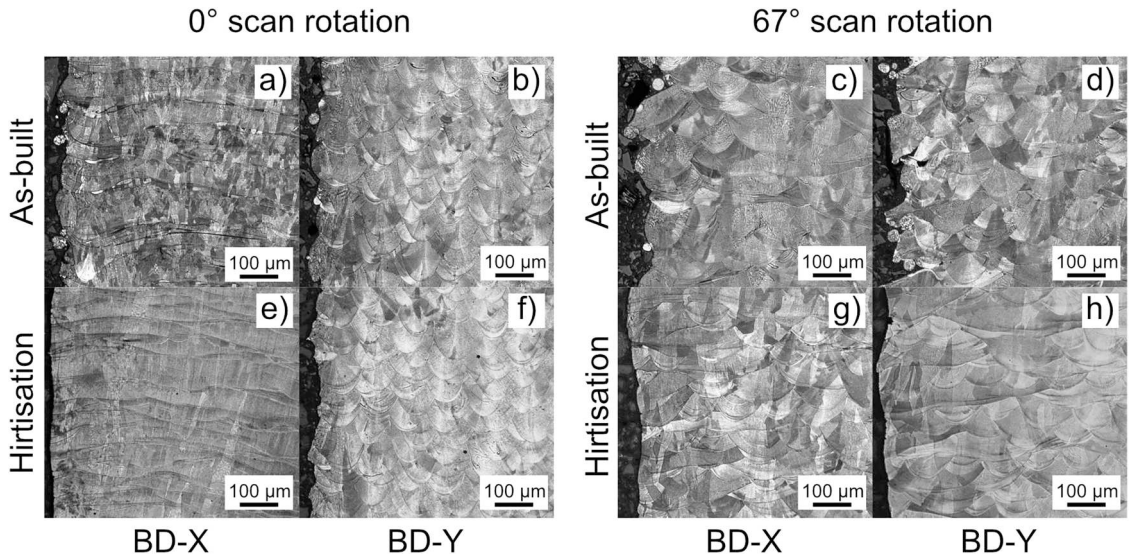

Figure 6. LOM micrographs of etched cross-sections of the 0° scan rotation: (a, b) in as-built condition and (e, f) after Hirtisation®. Similarly, the etched cross-sections of the 67° scan rotation are presented:(c, d) as built condition and (g, h) after Hirtisation®.

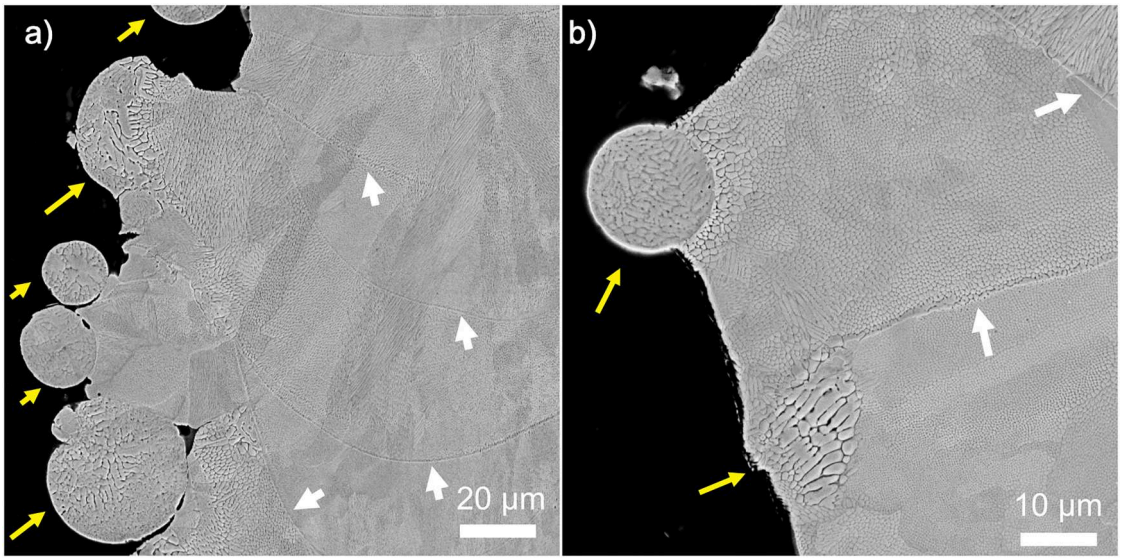

Figure 7. SEM images (a) and (b) of cross-sections of the as-built sample produced with 67° scan rotation: Yellow arrows indicate semi-sintered powder particles and white arrows indicate the boundaries of melt pools.

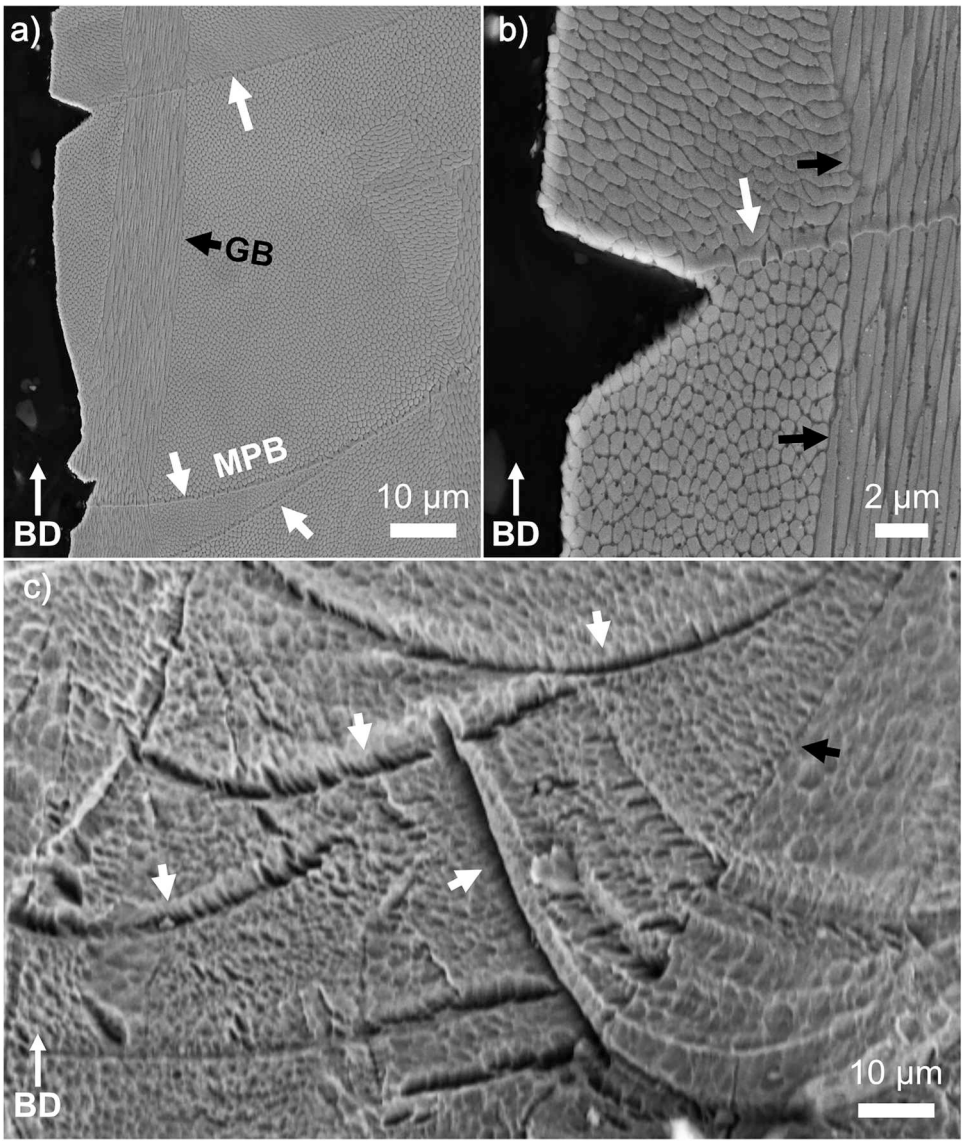

Figure 8. SEM images highlighting the microstructural features and regions preferentially attacked by the Hirtisation® process. White arrows indicate melt pool boundaries and black arrows grain boundaries. In (a) and (b) polished cross-sections of sample with 67° scan rotation, and (c) unpolished top surface of the same sample after Hirtisation®.

resulted in an anisotropic microstructure due to significant differences in solidification structure and thermal history. This is confirmed by the cross-section images for the 0° scan rotation sample in Figure 6 when comparing BD-X and BD-Y cross-sections. It is also evident from the images that all powder particles were removed by Hirtisation® (Figure 6(e–h)).

The SEM images in Figure 7 show the complex microstructure of the as-built sample produced with 67° scan rotation. Both partially and fully sintered powder particles are adhered to the surface (yellow arrows) contributing to local variations in microstructure. The powder consists of a cellular/dendritic structure of larger size compared to the fully melted subsurface consisting of fine networks of cells. These cells are organised in columnar grains stretching through several melt pool boundaries along the build direction (white arrows). For the Hirtisation® process this means that very different (local) microstructures are to be treated.

Figure 8(a and b) show the microstructure and surface features of the sample with 67° scan rotation after Hirtisation®. The semi-sintered powder particles are removed and sharp notches of up to ~10 µm in depth are now found in the vicinity of melt pool boundaries along the build direction. Figure 8(c) shows the same sample in unpolished condition, where the notches are seen near the melt pool boundaries. Melt pool boundaries are areas with high thermal stresses, non-equilibrium phases and segregation of solute elements.[19,20] Therefore, it is likely that these phase differences are easier to remove during the Hirtisation® process compared to other microstructural features. Previous work shows an improved corrosion behaviour towards pitting when the melt pool boundaries are removed by heat treatment above 950 °C.[19] Therefore, preferential material removal by Hirtisation® might not have occurred if the samples had been subjected to heat treatment before post-processing.

SEM images of the sample with 0° scan rotation show that the same features are also present there (Figure 9(a and b)). Sharp notches pointing inwards towards the melt pool boundaries can be clearly seen at a distance corresponding to the layer thickness of approximately 40 µm. Studies of the surface in top view (Figure 9(c and d)) show that melt pools/tracks, grain boundaries and cells are etched during the Hirtisation® process. These images highlight how the differences in melt pool characteristics yield an anisotropic surface pattern. This demonstrates the importance of the

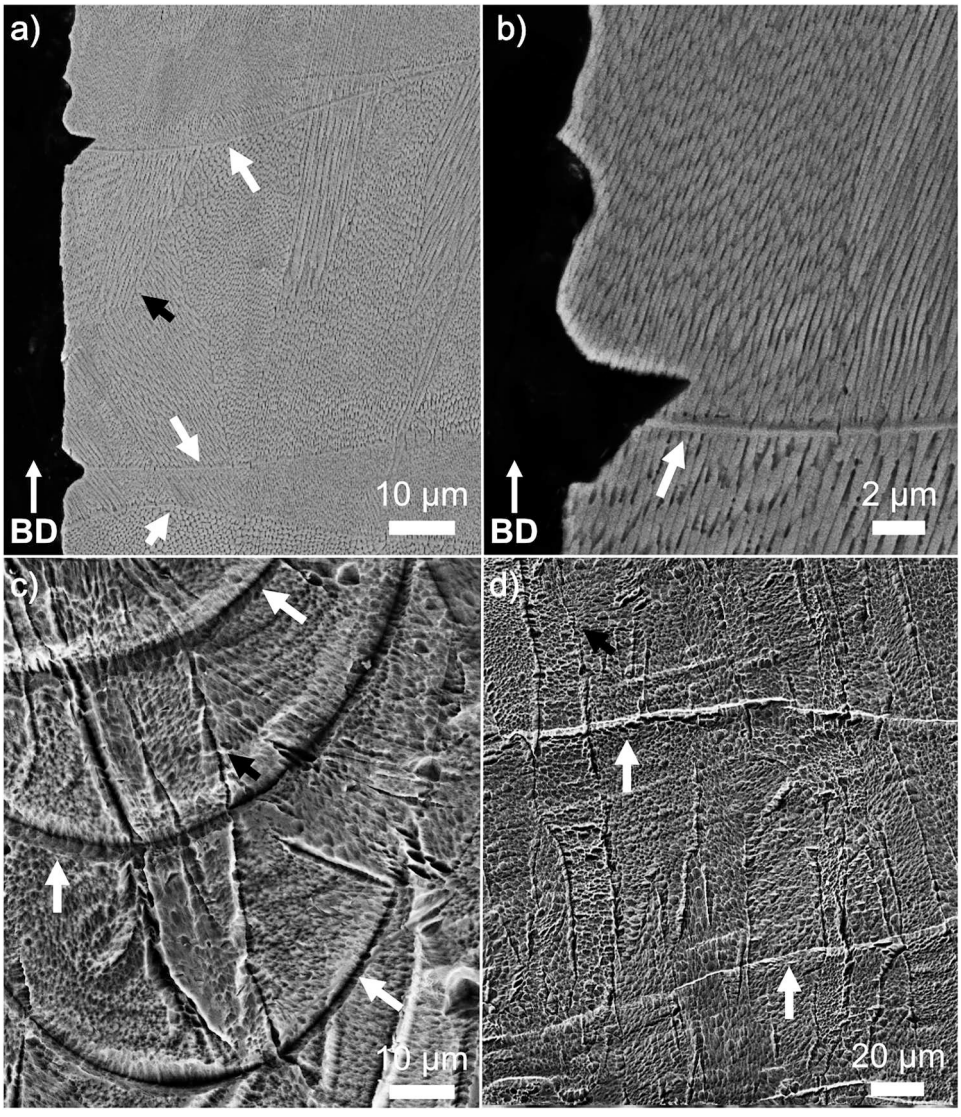

Figure 9. SEM images highlighting the microstructural features and regions preferentially attacked by the Hirtisation® process. White arrows indicate melt pool boundaries and black arrows grain boundaries. (a) and (b) show polished cross-sections of sample with 0° scan rotation, and (c) unpolished top surface of the same sample after Hirtisation®. (d) unpolished top surface of perpendicular cross-section.

different microstructural features on the material removal during Hirtisation®.

Conclusions

In this work, the effect of surface topography and microstructure on the material removal by the Hirtisation® process of PBF-LB processed 316L stainless steel was investigated. The study illustrated that surface topography as well as microstructure of PBF-LB produced samples affect the surfaces obtained after the Hirtisation® process. To obtain clear differences in microstructure, surface roughness and material removal, the standard 67° scan rotation was compared with the 0° scan rotation. Based on this work main findings can be summarised as follows:

- The surface roughness was significantly reduced by the Hirtisation® process. This was mainly due to the full removal of sintered/semi sintered powders on the as-built surfaces.
- The melt pool and melt track boundaries were preferentially attacked by the Hirtisation® process which led to notches of up to 10 µm in depth.
- Scan rotation has an effect on the final surface topography of samples post-processed by Hirtisation®. The 0° scan rotation yields lower surface roughness on one side.
- To achieve uniform surfaces after Hirtisation®, it is recommended that the initial surfaces are uniform for the entire part. This is achieved by a scan rotation of 67°, where the surfaces look similar in all cross-sections.

Acknowledgements

Paper based on a presentation given at the joint meeting 11th European Pulse Plating Seminar/EAST Forum 2024, 7-8th March 2024, Vienna, Austria.

Disclosure statement

No potential conflict of interest was reported by the author(s).

Funding

This work was performed in the frame of the ProThin project [Dnr: 2021-01273] and the Centre for Additive Manufacture – Metal (CAM^2), both supported by the Swedish Agency for Innovation Systems Vinnova.

ORCID

Uta Klement http://orcid.org/0000-0002-8945-3799

References

1. T. DebRoy, H. L. Wei, J. S. Zuback, T. Mukherjee, J. W. Elmer, J. O. Milewski, A. M. Beese, A. De Wilson-Heid and W. Zhang: Additive manufacturing of metallic components – process, structure and properties. *Prog. Mater. Sci.*, 2018, **92**, 112–224. doi:10.1016/j.pmatsci.2017.10.001.
2. J. Y. Lee, A. P. Nagalingam and S. H. Yeo: A review on the state-of-the-art of surface finishing processes and related ISO/ASTM standards for metal additive manufactured components. *Virtual Phys. Prototype*, 2021, **16**, 68–96. doi:10.1080/17452759.2020.1830346.
3. J. Gockel, L. Sheridan, B. Koerper and B. Whip: The influence of additive manufacturing processing parameters on surface roughness and fatigue life. *Int. J. Fatigue*, 2019, **124**, 380–388. doi:10.1016/j.ijfatigue.2019.03.025.
4. J. C. Snyder and K. A. Thole: Understanding laser powder bed fusion surface roughness. *J. Manuf. Sci. Eng., Trans. ASME*, 2020, **142**(7), 071003. doi:10.1115/1.4046504.
5. R. Wrobel, L. Del Guidice, P. Scheel, N. Abando, X. Maeder, M. Vassiliou, E. Hosseini, R. Spolenak and C. Leinenbach: Influence of wall thickness on microstructure and mechanical properties of thin-walled 316L stainless steel produced by laser powder bed fusion. *Mater. Des.*, 2024, **238**, 112652. doi:10.1016/j.matdes.2024.112652.
6. C. H. Yu, R. L. Peng, V. Luzin, M. Sprengel, M. Calmunger, J. E. Lundgren, H. Brodin, A. Kromm and J. Moverare: Thin-wall effects and anisotropic deformation mechanisms of an additively manufactured Ni-based superalloy. *Addit. Manuf.*, 2020, **36**, 101672. doi:10.1016/j.addma.2020.101672.
7. H. Fayazfar, J. Sharifi, M.K. Keshavarz and M. Ansari: An overview of surface roughness enhancement of additively manufactured metal parts: a path towards removing the post-print bottleneck for complex geometries. 2023, Springer, London. doi:10.1007/s00170-023-10814-6
8. C. Tang, K. Q. Le and C. H. Wong: Physics of humping formation in laser powder bed fusion. *Int. J. Heat Mass Transfer*, 2020, **149**, 119172. doi:10.1016/j.ijheatmasstransfer.2019.119172.
9. K. Artzt, T. Mishurova, P. P. Bauer, J. Gussone, P. Barriobero-Vila, S. Evsevleev, G. Bruno, G. Requena and J. Haubrich: Pandora's box-influence of contour parameters on roughness and subsurface residual stresses in laser powder bed fusion of Ti-6Al-4V. *Materials. (Basel)*, 2020, **13**, 1–24. doi:10.3390/ma13153348.
10. V. Sandell, J. Nilsson, T. Hansson, P. Åkerfeldt and M. L. Antti: Effect of chemical post-processing on surfaces and sub-surface defects in electron beam melted Ti-6Al-4V. *Mater. Characteris.*, 2022, **193**, 8–14. doi:10.1016/j.matchar.2022.112281.
11. E. Beevers, D. Neumayer, B. Bonvoisin, A. Brandão, S. Hansal, M. Doppler, T. Rohr and B. Van Hooreweder: Effect of Hirtisation treatment on surface quality and mechanical properties of AlSi10Mg samples produced by laser powder bed fusion. *Mater. Today Commun.*, 2024, **38**, 108042. doi:10.1016/j.mtcomm.2024.108042.
12. J. Berglund, J. Holmberg, K. Wärmefjord and R. Söderberg: Detailed evaluation of topographical effects of Hirtisation post-processing on electron beam powder bed fusion (PBF-EB) manufactured Ti-6Al-4V component. *Precision Eng.*, 2024, **85**, 319–327. doi:10.1016/j.precisioneng.2023.10.007.
13. R. N. Oosterbeek, G. Sirbu, S. Hansal, K. Nai and J. R. T. Jeffers: Effect of chemical-electrochemical surface treatment on the roughness and fatigue performance of porous titanium lattice structures. *Additive Manuf.*, 2023, **78**, 103896. doi:10.1016/j.addma.2023.103896.
14. Z. Que, T. Riipinen, P. Ferreirós, S. Goel, K. Sipilä, T. Saario, T. Ikäläinen, A. Toivonen and A. Revuelta: Effects of surface finishes, heat treatments and printing orientations on stress corrosion cracking behavior of laser powder bed fusion 316L stainless steel in high-temperature water. *Corr. Sci.*, 2024, **233**, 11211. doi:10.1016/j.corsci.2024.112118.
15. A. Leicht, C. H. Yu, V. Luzin, U. Klement and E. Hryha: Effect of scan rotation on the microstructure development and mechanical properties of 316L parts produced by laser powder bed fusion. *Mater. Charact.*, 2020, **163**, 2–10. doi:10.1016/j.matchar.2020.110309.
16. Hirtisation Surface Treatment of Printed Metal | RENA: n.d., https://www.rena.com/en/technology/process-technology/hirtisation (accessed August 5, 2024).
17. F. Cabanettes, A. Joubert, G. Chardon, V. Dumas, J. Rech, C. Grosjean and Z. Dimkovski: Topography of as built surfaces generated in metal additive manufacturing: a multi scale analysis from form to roughness. *Precis. Eng.*, 2018, **58**, 249–265. doi:10.1016/j.precisioneng.2018.01.002.
18. SIS (Swedish Standards Institute): *Svensk Standard, Ss*, 2018, **812310** (2014), 24. www.sis.se.
19. M. H. Ghoncheh, A. Shahriari, N. Birbilis and M. Mohammadi: Process-microstructure-corrosion of additively manufactured steels: a review. *Critical Rev. Solid State Mater. Sci.*, 2023, **49**(4), 607–717. doi:10.1080/10408436.2023.2255616.
20. M. Moyle, C. Ledermueller, Z. Zou, S. Primig and N. Haghdadi: Multi-scale characterisation of microstructure and texture of 316L stainless steel manufactured by laser powder bed fusion. *Mater. Charact.*, 2022, **184**, 111663. doi:10.1016/j.matchar.2021.111663.